

# Computerized decision support in liver steatosis investigation

Simona Moldovanu, Luminita Moraru, Dorin Bibicu

**Abstract**—Fractal analyses, Euler number and RF5 texture parameter have been successfully applied in the analysis of many types of ultrasound images. All features have been extracted from binary images. We focused our study on liver ultrasonic (US) images. The US experimental images were divided in two groups: healthy liver US images and steatosis US liver images. The goals of this study are both to develop an automatic system in order to investigate the correlation between certain features and the optimum threshold and to take into account an automatic decision support of the studied pathologies using the correlation results. The tool for this analysis is an Automatic Correlation System (ACS) that allows us to investigate the correlation between the optimum threshold (OT), fractal dimension (FD), Euler number (EN) and RF5 parameter. Finally, based on correlation results, the ACS software tool is extended in a Computer Automatic Diagnosis System (CADi), in order to provide a reliable discriminator tool of the liver steatosis as support for medical diagnosis. The features have been extracted from different regions of interest (ROIs) cropped in both classes of liver original images (healthy and fatty). In order to obtain OT, each selected ROI was transformed from a gray level image into a binary image using the Otsu method. The ACS proposed system uses the Box Counting Method (BCM), the Euler algorithm based on concavity and convexity and the algorithm which allows the obtaining of the iso-segments matrix. The Pearson coefficient is used to correlate the calculated FD, EN and RF5 data for each characteristic OT for both liver classes. The CADi software was developed using the artificial neural networks. Finally we investigated the CADi efficiency.

**Keywords**—ultrasound liver images, optimum threshold and image features, Pearson's correlation, CADi software.

Manuscript received October 9, 2007; Revised version received March 4, 2008. This work was supported in part by the Project SOP HRD -TOP ACADEMIC - 107/1.5/S id 76822 of Dunarea de Jos University of Galati, Romania.

S. Moldovanu is with the Faculty of Sciences and Environment, Physics Department, University of Galati 47 Domneasca St., 800008 Galati Romania (e-mail: [Simona.Moldovanu@ugal.ro](mailto:Simona.Moldovanu@ugal.ro)).

L. Moraru., is with the Faculty of Sciences and Environment, Physics Department, University of Galati 47 Domneasca St., 800008 Galati Romania (corresponding author, e-mail: [luminita.moraru@ugal.ro](mailto:luminita.moraru@ugal.ro)).

D. Bibicu is with the Faculty of Sciences and Environment, Physics Department, University of Galati 47 Domneasca St., 800008 Galati Romania (e-mail: [Dorin.Bibicu@ugal.ro](mailto:Dorin.Bibicu@ugal.ro)).

## I. INTRODUCTION

Medical European studies have shown that a percent varying between 20% -30% of the population from developed countries is suffering from fatty liver disease, also known as steatosis [1]. This disease represents all the accumulated triglycerides in the liver tissue and in severe cases the fat proportion is more than 40% of the liver's weight. Normally, the fat proportion is 3%.

The fatty liver or steatosis liver appears in obese people and it is produced by an abnormal lipid within liver. At present physicians diagnose patients with fatty liver based on visual observation of ultrasound images. Increased parenchymal echogenicity is a criterion for diagnosing fatty liver. The visual features of a fatty liver noticed by human eye from ultrasound images are: bright pattern, vascular blurring and deep attenuation. If the liver image is much brighter it is fatty. Texture-based method is an essential visual property in tissue characterization and in pathological structures recognition.

As a result of the desire to find a gold standard method to diagnose this disease, the research studies described in [2] have presented various methods to classify the prevalence of fatty liver disease. The approach and results are different depending on the utilized methods. For magnetic resonance imaging the score is between 31 to 34% [3], for liver biopsy is from 15 to 39% [4], and for ultrasonography is from 16 to 29% [5]. The diffuse liver disease and the liver cancer were investigated based on an exploring of the texture parameters [6].

In the last years many algorithms that quantify the textural properties of the liver ultrasound image have been developed. We mention the co-occurrence matrices [7], [8], Gabor filters [9] and recently, Lee et al. developed an unsupervised segmentation algorithm for liver ultrasonic images based on the multi-resolution fractal feature vector [10], [11].

Our start idea was that the performance and utility of the analysis would be improved by using a combination of textural parameters. We proved through study that this statement is especially true when there are combined features which described different aspects of texture: the self-similarity of the biological objects, topological of the image content and the gray level value in a certain direction.

In this respect, we have developed the ACS in order to determine the correlation between certain features extracted from US images. The features EN, FD and RF5 were extracted

from US liver image and this topic is presented in detail in the next sections. These texture analysis techniques are based on space domain. The ACS gives the possibility to verify whether various features are compatible and also their correlation. The database of the ACS can be updated anytime. The current database comprises 50 ROIs cropped from two liver classes (healthy and fatty) represented in US images. Each ROI was used to extract the FD and EN features. Then these features were correlated using the Pearson's correlation coefficient. The correlation stage is a very important step because it allows analyzing the correlations between features. Using Pearson's coefficient values, we can decide whether the threshold level influences FD, EN, and RF5.

In carrying out the correlation features, the main step represents the choice of the best thresholding method. The method implemented in ACS was Otsu's method, which chooses the optimal threshold to minimize the intra-classes variance of the black and white pixels. Then, the correlations results, the decision parameter RF5 feature and the artificial neural networks were used to develop the CADi system able to automatically recognize the steatosis liver texture as characteristic of the image.

In the US steatosis liver automatic investigation domain our contribution was the study regarding the correlation of the binarization threshold with the image features and a new CADi approach has been developed for steatosis liver disease detection.

The paper is organized as follows: section 1 is an introduction in our study, in section 2 we presented the theoretical methods used, section 3 describes the experimental methods, section 4 provides the results and discussions. Finally, the concluding remarks are presented.

## II. UNDERLYING THEORY

### A. Fractal Dimension

The fractal concept was proposed by Mandelbrot [12], but this notion was defined by Lauwerier [13]. In a review about applying fractals in medical image analysis, Lopes and Betrouni [14] mentioned that the fractal geometry in medical image analysis used the self-similarity of the biological objects. They carried out a review about the fractal and multi-fractal analysis of medical signal, where the Hausdorff-Besicovitch dimension is defined as the logarithmic ratio between the number of an object's internal homotheties N and the reciprocal of the common ratio of the homothety r:

$$D_h = \frac{\ln(N)}{\ln\left(\frac{1}{r}\right)} \quad (1)$$

FD is computed using the BCM method defined by Russel et al. [15] and it has the expression:

$$D_h = -\lim_{r \rightarrow 0} \frac{\log N(r)}{\log r} \quad (2)$$

where N(r) is the number of the boxes needed to completely cover the binarization image.

### B. Euler Number

L. Xiaozhu et al., in their paper [16], defined the Euler number as "one of the most important characteristics in topology". In bi-dimensional digital images, the Euler number is locally computed. In order to compute the EN, a number of algorithms have been developed such as those presented in [17], where the algorithm is based on the graph theory, divide-and-conquer paradigm in [18], and binarization [19] or on curvature (convexity and concavity) in [20].

In our study we used the curvature algorithm. In 2D images, the Euler number (EN) is defined as the difference between the number of connected components C and the number of holes H.

$$EN = C - H \quad (3)$$

In the case of binary images contained in our database, the Euler number has been computed after the thresholding operation of the input gray value image had been performed. For this operation we used the optimal threshold value provided by the Otsu method [21]. The high level of noise has a decisive impact on EN, leading to large positive and negative values.

### C. Iso-segment matrix

The iso-segment matrix (or run-length matrix) is proposed by M. Galloway [22] in order to realize the extraction of the texture features. The iso-segment matrix has been successfully applied in medical imaging investigation [23], [24]. In imaging, the iso-segment (or gray level run) is defined as a set of consecutive and collinear pixels which have the same gray level in a certain direction. The iso-segment length is equal to the number of iso-segment pixels. The number of rows of the iso-segment matrix is equal to the number of the gray levels for each analyzed ROI. In our study, the used matrix has two rows because the binarized images have two gray levels (white=1 and black=0). There are many texture descriptors corresponding to the iso-segment matrix such as: Niz (the number of iso-segments), RF1 (the proportion of short iso-segments), RF2 (the proportion of long iso-segments), RF3 (the gray-level heterogeneity), RF4 (the iso-segments length heterogeneity) and RF5 (the proportion of iso-segments). We investigated the correlation between OT and RF5 parameter because this parameter takes into accounts both the size and texture characteristics. The parameter RF5 is defined by the expression:

$$RF5 = \frac{N_{iso}}{N_{reg}} \quad (4)$$

where  $N_{iso}$  represents the number of the iso-segments and  $N_{reg}$  is the number of pixels into image.

#### D. Thresholding

The Otsu method is frequently used in various fields and its goal is to convert a grayscale image into a binary image for an optimal threshold OT. The method was proposed in [25] and the partition of the pixels into two classes is based on discriminatory analysis.

In our study, we apply the Otsu threshold algorithm for each cropped ROI belonging to the two liver classes in order to determinate the OT [21]. The threshold values are between 0 and 1. The binarization techniques consist in the transformation of the grayscale images in atonal images. All pixels with intensity less than a certain threshold are set to 0 (color black) and the rest of the pixels are set to 1 (color white).

#### E. Statistical Analysis

For many types of correlation, the Pearson's correlation coefficient (PCC), relation (5), is the most widely used instrument [26], [27]. In the relation (5), N represent the number of the experiments and  $x_i$ ,  $y_i$  the experimental values.

$$PCC = \frac{\sum_{i=1}^N (x_i - \bar{x})(y_i - \bar{y})}{\sqrt{\sum_{i=1}^N (x_i - \bar{x})^2 (y_i - \bar{y})^2}} \quad (5)$$

The values of PCC coefficient are between -1 and +1. A PCC value equal to 0 indicates a complete lack of correlation between the variables. A PCC negative value indicates a negative correlation and when PCC has a positive value then there is a positive correlation between the variables. In the statistical theory, if the PCC value is in 0 and 0.2 interval, the correlation is very weak; for 0.2 and 0.4 interval, there is a weak correlation; for range 0.4 to 0.6 it is a medium or good correlation; for range 0.6 and 0.8 it is a high correlation between measured parameters and, finally, if the PCC value is between 0.8 and 1, there is a very high correlation.

In our correlation study, the dimensions (OT/FD), (OT/EN) and (OT/RF5) have been used. The PCC value of -1.00 indicates a perfect negative correlation and the +1.00 indicates a perfect positive correlation [28].

#### F. CADi System

The Computer Aided Diagnosis System (CADi) was developed in order to accurately accomplish the discriminatory task of different liver status. The overall performance of the radiologists' diagnostic towards accurate detection and precise characterization of potential abnormalities in US images is influenced by the radiologists' perception, experience, even their fatigue and also, the quality of the acquisition image [29].

In the specialized literature, many CADi systems were developed in order to investigate the diseases by analyzing the US images [30]-[32].

In order to eliminate the human diagnostic deficiencies the automatic diagnosis systems are widely used. The proposed CADi software is a learning machine that is previously trained using two correct data sets. The classification software tool is based on the artificial neural networks principle. The automatic classification and recognition efficiency of the CADi software was investigated by using the sensitivity and the specificity rates (see the relations (4) and (5)) [33], [34] and the correct classification rate (CCR) (relation 6) [35]. The sensitivity and the specificity rates handle with True-Positive TP (presence of malignancy correctly diagnosed), False-Positive FP (healthy liver was incorrectly diagnosed as steatosis liver), True-Negative TN (absence of malignancy correctly diagnosed) and False-Negative FN (steatosis liver was incorrectly diagnosed as healthy). CCI is the number of the correct classified images and TI is the total number of the experimental images.

$$Sensitivity = \frac{TP}{TP + FN} \quad (6)$$

$$Specificity = \frac{TN}{TN + FP} \quad (7)$$

$$CCR = \frac{CCI}{TI} \quad (8)$$

### III. EXPERIMENTAL METHODS

In this study, the hardware experimental environment was Intel (R) Core (TM) 2 Duo CPU T 5900, 2.20 with 3G RAM, and the Toolbox Processing Image from the language of technical computing MATLAB R2009a and statistical application SPSS version 17.0 were used. The procedural flowchart of the ACS-CADi is displayed in Fig. 1 and the graphic user interface GUI is presented in Fig. 2.

This diagram is easy to use and the blocks are grouped as following: the block "Acquisition" presents the acquisition of the liver ultrasound (US) images; the block "load liver" presents the input of liver US images in the ACS-CADi; the block "Cropping US" contains the interactive functions of the cropped ROIs from original US image; the block "Extracting cropping" is a function that allows to delimitate the ROIs; the block "Computing optimum threshold" contains the Otsu algorithm to compute the OT; the block "Transforming in binary image" contains the function which transforms a gray level image into a binary image in accordance with OT; the block "FD" implements the BCM to compute the fractal dimension; the block "EN" implements the concavity and convexity algorithms to compute EN; the block "RF5" gets the iso-segment matrix to compute the RF5 parameter; the blocks "Correlation features" uses Pearson's coefficient to correlate the OT/FD, OT/EN and OT/RF5; and finally the Diagnosis block discerns and recognizes the healthy or the steatosis pathology.

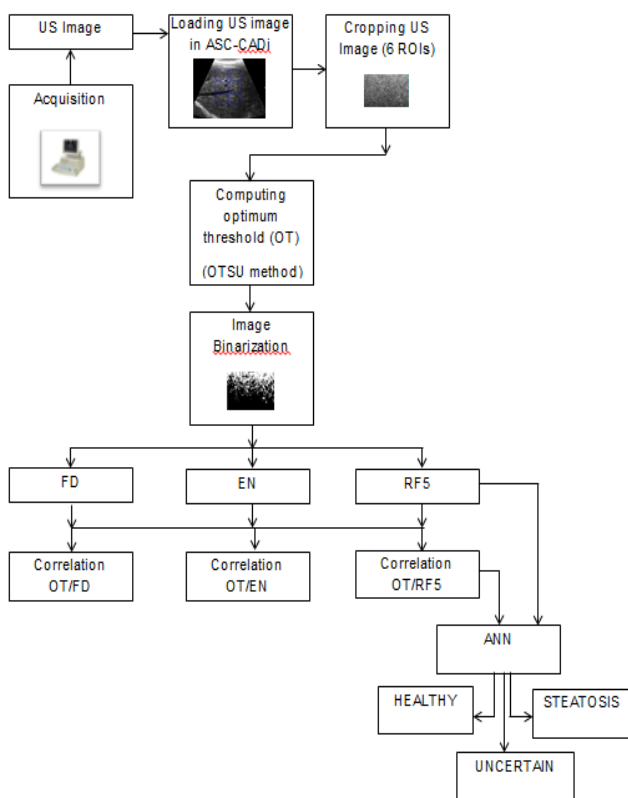


Fig.1 The proposed diagnostic flowchart of ACS-CADI

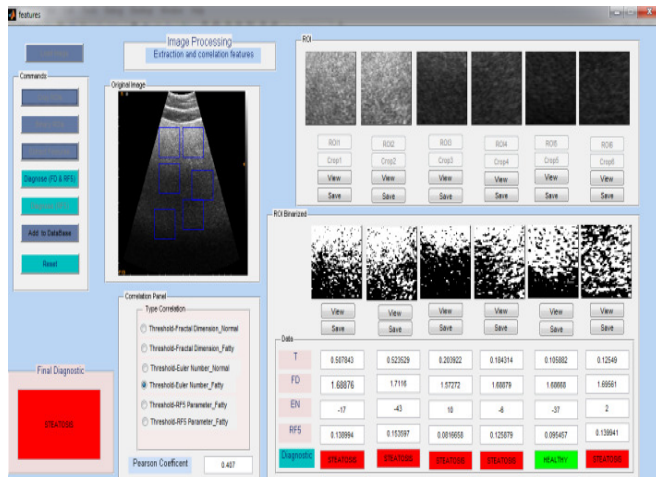


Fig. 2 Graphic User Interface of the ACS-CADI system software

The clinical study involves 20 patients, divided into two equal groups: 10 of them presented a healthy liver and 10 of them are diagnosed with steatosis. Median age is 60 years for the class of fatty liver and 56 years for the class of healthy liver. The experimental US images (Figs. 3 (a), (b)) are acquired using the scanning systems SLE-401 and the curvilinear probe with transducer variable frequency of 3–6 MHz. The liver US images used in this research were captured from the same machine and were digitized in the format matrix 512 x 524 pixels and of 256 grey-level resolutions.

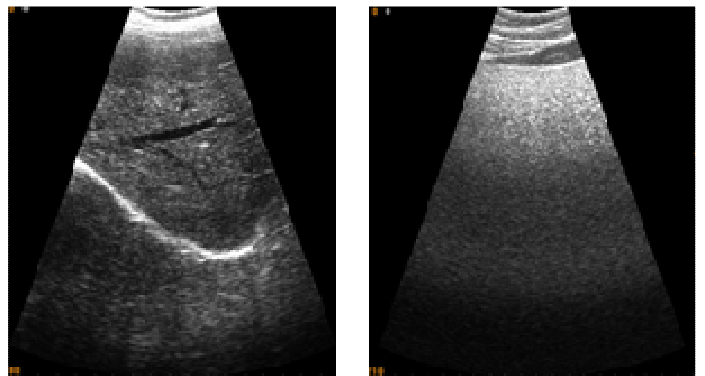


Fig. 3 (a) US healthy liver

Fig. 3 (b) US steatosis liver

Using this system, a number of 25 squares ROIs, with 85 pixel side, of each liver class was cropped. Each ROI provided the OT, FD, EN and RF5 features (see Table I). The correlation values (see Table II) were calculated using the SPSS statistical program, and scatter plots (see Figs. 7) were generated using the same software.

In order to develop the CADi system, the RF5 texture feature has been chosen as decision parameter. The CADi software used artificial neural networks techniques. The ANN is employed to classify pattern based on learning from examples and it is trained using 6 ROIs cropped from the analyzed US image (Fig. 4). The used ROIs are squares with 85 pixels side and can be manually positioned in the US image area. It is important that the ROIs do not overlap on the portal or suprahepatic vein. The incorrectly positioned ROIs can lead to wrong decisions.

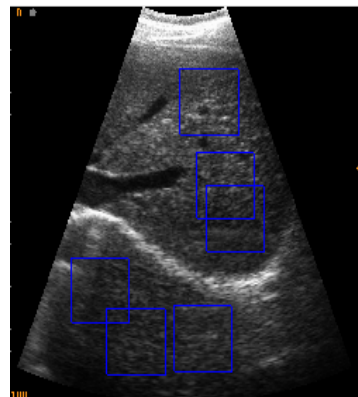
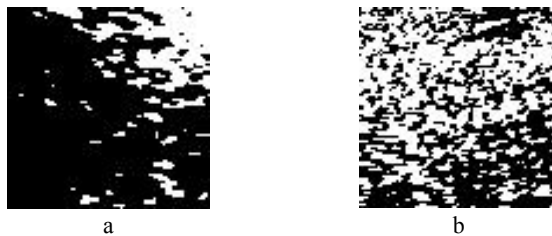


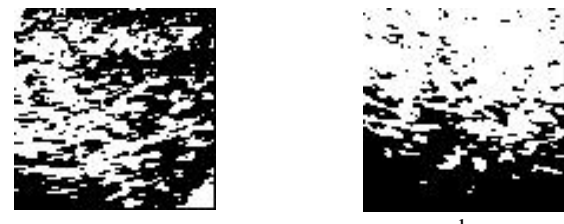
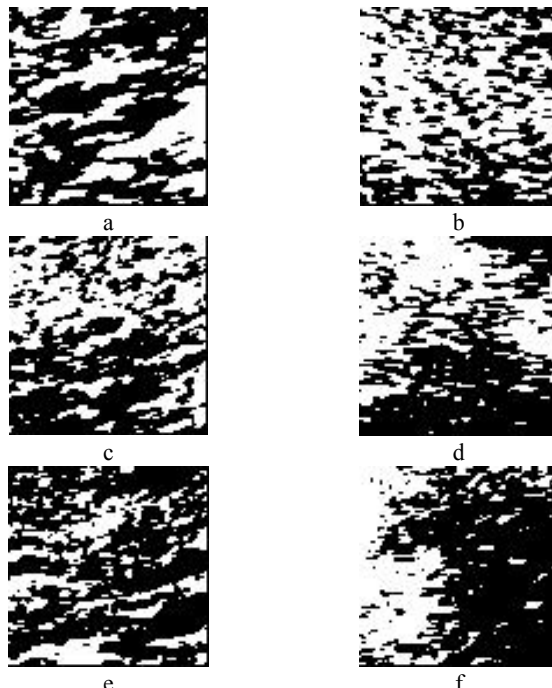
Fig. 4 The six ROIs used in diagnosis process

Since we handled a large number of the computed features, we encountered difficulties in validating their discriminative power, so we looked for a feature selection procedure. Our previous work shows that the value of the binarization threshold affects the accuracy of the RF5 value. For threshold values lower than 0.1, each and every ROI are members of the healthy class and none of them can be found in the steatosis class. For threshold values higher than 0.5, all ROIs belong to the steatosis class and zero ROIs are from healthy class. Therefore, if the investigated ROI have the binarization threshold less than 0.1, the associate classification is NEGATIVE, if the value of the binarization threshold is more

than 0.5, the associate classification is POSITIVE. For the intermediated threshold values, we considered four intervals associated to threshold values ranges 0.1 to 0.2, 0.2 to 0.3, 0.3 to 0.4, 0.4 to 0.5. The ROIs were investigated taking into account the threshold value and the associate threshold range. Also, for each defined range the neural network was trained. The four neural networks (ANN1, ANN2, ANN3 and ANN4) are feed-forward network single layer perceptron. The features vector is done through the RF5 value (see Table 3). A training images set for healthy class and a training images set for steatosis class were identified for each neural network. Figure 5 (a) presents an example of ROI cropped from healthy liver image which was binarized at a threshold less than 0.1. Figure 5 (b) presents a ROI cropped form a steatosis liver image but it was binarized at a threshold higher than 0.5. In the figures 6 (a)-(h), some examples of images used in training process are presented for four neural networks.



Figs. 5 (a) Binarized ROI of healthy liver at a threshold <0.1; (b) Binarized ROI of steatosis at a threshold > 0.5.



Figs. 6 (a) Training healthy image data sets for ANN1; (b) Training steatosis image data sets for ANN1; (c) Training healthy image data sets for ANN2; (d) Training steatosis image data sets for ANN2; (e) Training healthy image data sets for ANN3; (f) Training steatosis image data sets for ANN3; (g) Training healthy image data sets for ANN4; (h) Training steatosis image data sets for ANN4.

#### IV. RESULTS AND DISCUSSIONS

Table I presents some examples of the texture feature values calculated for 5 ROIs from healthy liver class and for 5 ROIs from steatosis liver class.

Table I Examples of the texture features values

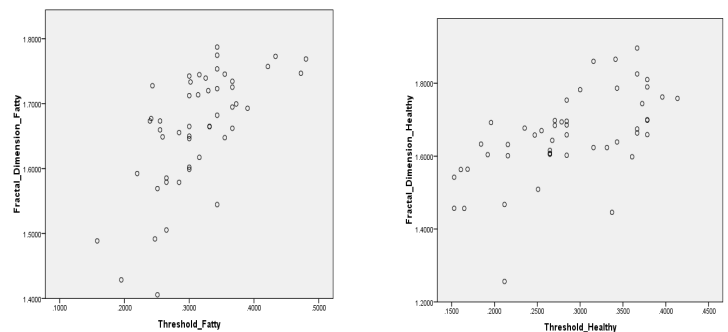
No.	Healthy liver				Steatosis liver			
	OT	FD	EN	RF5	OT	FD	EN	RF5
1	0.37	1.57	76	0.122	0.27	1.59	16	0.080
2	0.22	1.65	17	0.130	0.50	1.68	-17	0.130
3	0.26	1.63	26	0.122	0.20	1.57	10	0.081
4	0.33	1.60	37	0.118	0.31	1.59	32	0.085
5	0.15	1.65	20	0.106	0.12	1.69	2	0.139

The calculated Pearson correlation values are presented in Table II.

Table II. Pearson's coefficient for each correlation type

	Correlation type	PCC
Healthy liver class	OT/FD	0.605
	OT/EN	-0.133
	OT/RF5	-0.460
Fatty liver class	OT/FD	0.656
	OT/EN	-0.104
	OT/RF5	0.510

According to the scatter plots displayed in figures 7a and 7b, a linear correlation is observed. The same tendency is observed for the scatter plot shown in figure 7e. In the graphs 7a and 7b both the (OT /FD) dimensions increase. The scatter plots displayed in figures 7c and 7d are rather uncorrelated.



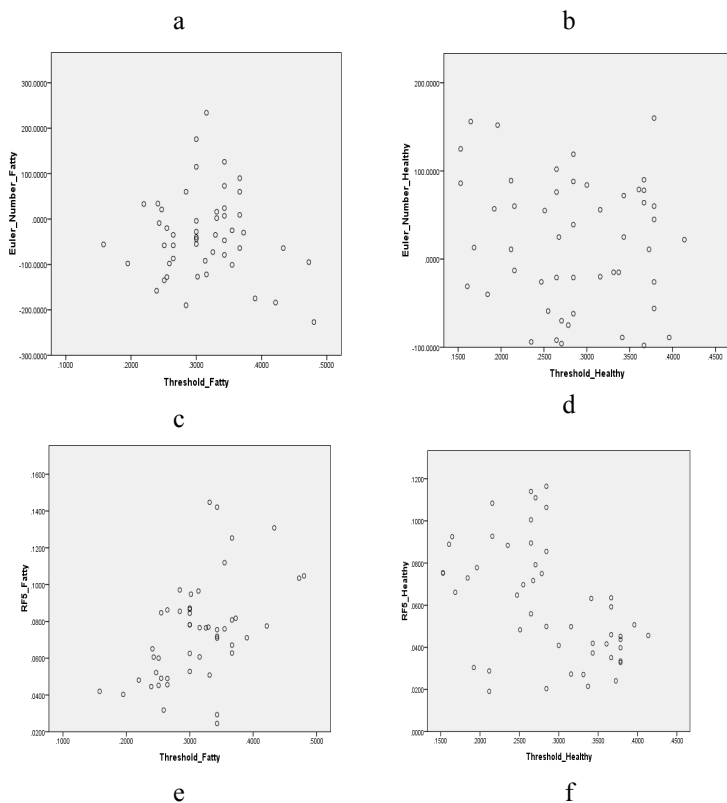


Fig. 7 Scatter plots showing the correlation between: (a) OT/ FD for fatty liver class; (b) OT/ FD for healthy liver class; (c) OT/ EN for fatty liver class; (d) OT/ EN for healthy liver class; (e) OT/ RF5 for fatty liver class; (f) OT/ RF5 for healthy

For the healthy liver class, the calculated OT/FD correlation has the value of  $PCC=0.605$ . The qualitative description is “moderate positive”, namely a positive association between the variables. The OT/EN correlation for the same class provides  $PCC = -0.133$ . The qualitative description is “little or no association”. The OT/RF5 correlation for the same class provides  $PCC = -0.460$ . The qualitative description is “moderate negative”.

For the fatty liver class, the OT/FD correlation provides a  $PCC = 0.656$  and the qualitative description is “moderate positive”. The correlation OT/EN for the same class provides  $PCC = -0.104$ ; the qualitative description is “little or no association”. The correlation OT/RF5 for the same class provides  $PCC = 0.510$ ; the qualitative description is “moderate positive”.

In case of healthy liver class, 36.6% of the variation of the FD feature and 21.1% of the variation of the RF5 feature can be explained by using the variation of the OT features. But only 5.2% of the variation of the EN feature can be explained using the same variation of OT, so the EN cannot be a really correlated feature. For the fatty liver class the features are better correlated, namely 43% of the FD variation and 26 % of the RF5 variation can be explained through the variation of OT feature. On the other hand, the EN feature is clearly uncorrelated to the OT ( $PCC$  is approximately 1%). The lower and higher values of EN are associated with both higher and lower optimal threshold OT values.

There is a significant positive correlation between FD and OT for both healthy and fatty liver classes, significant positive correlation between RF5 and OT for fatty liver, significant negative correlation between RF5 and OT for healthy liver, but there is a little or no correlation between EN and OT for both classes. The OT/FD correlation for fatty liver is slightly higher than the OT/FD for healthy liver which reflected a statistical difference between the two classes. Fractal dimension and RF5 texture parameter can be a useful tool to differentiate a fatty liver from a healthy liver, while the Euler number is overestimated. However, our goal was to combine the FD, RF5 and EN as parallel features to discriminate between liver diseases and to correlate these features with the OT values. This combination has a good sensitivity but a poor positive predictive value when the EN feature is used. Even if the FD seems to be more useful than RF5, in our opinion all features should be estimated whenever possible.

In table III, there are presented some examples of the feature vectors values corresponding to the four considered threshold intervals and to the neural networks associated.

Table III Examples of the feature vectors values corresponding to the four threshold intervals (neural networks associated)

Interval	Healthy class RF5	Steatosis class RF5
0.1 to 0.2	0.112	0.145
	0.105	0.133
	0.090	0.125
0.2 to 0.3	0.130	0.069
	0.146	0.100
	0.164	0.069
0.3 to 0.4	0.122	0.084
	0.132	0.100
	0.119	0.650
0.4 to 0.5	0.107	0.124
	0.104	0.120
	0.111	0.123

For an investigated US image by the instrumentality of CADi system, the final diagnostic is given by the predominant result provided by the six considered ROIs in image analysis. The final classification can be either NEGATIVE or POSITIVE. If the intermediary results are in equal proportion (three positive and three negative) the final decision is UNCERTAIN.

For each US image, three attempts were made as the ROIs were positioned in various positions. Therefore, we obtained 30 final results for each US set.

In table IV we present the values of final classification rate of the experimental set: TN represents the number of healthy cases correctly diagnosed, TP gives the number of steatosis cases correctly diagnosed, FP is the number of the healthy cases with incorrect classification and FN represents the number of the steatosis cases incorrectly recognized and U is

the number of the uncertainty cases.

In order to design an effective classification system, the main goal is to decrease the rate of misclassification. Here we are targeted on the false negative rate FN. A high FN rate could lead both to underestimate the severity of disease and to a wrong clinical approach if a CADi system is used by physicians.

**Table IV Diagnostic results and final classification rate**

Healthy class			Steatosis class		
TN	U	FP	TP	U	FN
23	6	1	23	5	2

Table V presents the efficiency of CADi software application CCR, the sensitivity and specificity of statistical parameters. In our statistical analysis we do not take into account the uncertainty values because they do not correctly fit the experimental image in a pathological class.

**Table V Performance of the CADi application**

CCR	Sensitivity	Specificity
94 %	96 %	92 %

Finally, we note that the efficiency of the CADi system is closely related to the proper choice of the ROIs that constituted the training sets.

## V. CONCLUSION

The aim of this study was to compare various features for discriminate between normal and abnormal livers. This paper introduces the problem of grouping patients according to their OT, FD, EN and RF5 parameters of liver ultrasound images. Based on the first results presented in this paper, the proposed method has provided efficient results for distinguishing and classifying between normal and steatosis liver.

This study is a benchmark to estimate the correlations between four features using the Pearson's correlation coefficient. An automatic correlation system has been developed in order to compute the OT, FD, EN and RF5 features and the OT/FD, OT/EN and OT/RF5 correlations. After the analysis of these correlations, we can conclude whether the OT value influences the values of the other three features.

The ACS is an original strategy, which leads to unbiased knowledge and can be used and/or adapted by choosing the correlated features in a CADi (Computer-Aided Diagnosis System).

According to the results of this study, the OT predictor variable from which we transform the gray level image into a binary image correlates well with the FD and the RF5 predicted variables; it has a weak correlation with RF5 predicted variable and has a little or no correlation with EN predicted topological feature.

The CADi software was developed using the RF5 feature as decision parameter and provided the NEGATIVE, POSITIVE

or UNCERTAIN recognition status. The CADi software has a very good efficiency and can be used to assist the students or the novice physicians in the liver pathology investigation.

This work could enhance the textural analysis approach and also highlights the features that should be considered challenging tasks in further liver assessments by using automated methods and confirms that the ACS can bring a considerable contribution in choosing the texture features useful for the analysis of US liver images.

Since the fatty liver presents many types (such as mild, moderate and severe etc.), in the future we intend to extend the CADi study based on the neural networks techniques and the analysis of the white and black iso-segments proportion, following the idea that the fat proportion could be correlated to the RF5 feature).

## ACKNOWLEDGMENT

The authors would like to thank the Project SOP HRD-EFICIENT 61445/2009 and the Project SOP HRD -TOP ACADEMIC - 107/1.5/S id 76822 of Dunarea de Jos University of Galati, Romania.

## REFERENCES

- [1] D. Preiss, N. Sattar, "Non-alcoholic fatty liver disease: an overview of prevalence, diagnosis, pathogenesis and treatment considerations", Clinical Science, Vol.115, No.5, 2008, pp.141-150.
- [2] JL. Narciso-Schiavon, L de L Schiavon, RJ. Carvalho-Filho, DY. Hayashida, JH. Wang, TS. Souza, CT. Emori, ML. Ferraz, AE. Silva, "Clinical characteristics associated with hepatic steatosis on ultrasonography in patients with elevated alanine aminotransferase", Sao Paulo Med J., Vol. 128, No.6, 2010, pp. 342-347.
- [3] J. Browning, LS. Szczepaniak, R. Dobbins, "Prevalence of hepatic steatosis in an urban population in the United States: impact of ethnicity", Hepatology, Vol. 40 , No.6, 2004, pp.1387-1395.
- [4] M. Hilden, P. Christoffersen, J.B. Dalgaard, "Liver histology in a 'normal' population examinations of 503 consecutive fatal traffic casualties", Scand J Gastroenterol, Vol.12, No.5, 1977, pp. 593-597.
- [5] G. Bedogni, L. Miglioli, F. Masutti, "Prevalence of and risk factors for nonalcoholic fatty liver disease: the Dionysos nutrition and liver study", Hepatology, Vol. 42, No.1, 2005, pp. 44-52.
- [6] D. Mitrea, S. Nedevschi, E. Cenan, M. Lupșor, R. Badea, "Exploring Texture-Based Parameters for Noninvasive Detection of Diffuse Liver Diseases and Liver Cancer from Ultrasound Images", Proceedings of the 8th WSEAS International Conference on Mathematical Methods and Computational Techniques in Electrical Engineering, 2006, pp. 259-265.
- [7] Y. Wang, K. Itoh, N. Taniguchi, H. Toei, F. Kawai, M. Nakamura, K. Omoto, K. Yokota, T. Ono, "Studies on tissue characterization by texture analysis with co-occurrence matrix method using ultrasonography and CT imaging", Journal of Medical Ultrasonic, Vol. 29, No. 4, 2006, pp. 211-223.
- [8] J.C. Felipe, A.J.M. Traina, C.Jr. Traina, "Retrieval by content of medical images using texture for tissue identification", Proceedings 16th IEEE Symposium Computer-Based Medical Systems, 2003, pp. 175 - 180.
- [9] C.C. Lee, S.H. Chen, H.M. Tsai, P.C. Chung, Y.C. Chiang, "Discrimination of Liver Diseases from CT Images Based on Gabor Filters", 19th IEEE Symposium on Computer-Based Medical Systems, 2006, pp. 203-206.
- [10] W.L. Lee, Y.C. Chen, K.S. Hsieh, "Ultrasonic Liver Tissues Classification by Fractal Feature Vector based on M-band Wavelet Transform", IEEE Trans. Medical Imaging, Vol. 22, No.3, 2003, pp. 382-392.

- [11] W. Lee, Y. Chen, K. Hsieh, "Unsupervised segmentation of ultrasonic liver images by multiresolution fractal feature vector", *Information Sciences*, Vol.175, No.3, 2005, pp. 177-199.
- [12] B.B. Mandelbrot, "The Fractal Geometry of Nature", San Francisco, 1983.
- [13] H. Lauwerier, "Fractals: Endlessly Repeated Geometrical Figures", Princeton , 1991.
- [14] R. Lopez, N. Betrouni, "Fractal and multifractal analysis: A review, *Medical Image Analysis*", Vol. 13, No.4, 2009, pp. 634-649.
- [15] D. Russel, J. Hanson, E. Ott, "Dimension of strange attractors", *Physical Review Letters*, Vol.45, No.14, 1980, pp. 1175-1178.
- [16] L. Xiaozhu, S. Yun, J. Junwei, W. Yanmin, "A proof of image Euler Number formula", *Science in China Information Sciences*, Vol.3, 2006, pp. 364-371.
- [17] M.H. Chen, P.F. Yan, "A fast algorithm to calculate the Euler number for binary images", *Pattern Recognition Letters*, Vol.8, No.5, 1988, pp. 295-297.
- [18] S. Deyy, B.B. Bhattacharya, M.K. Kundu, "A Fast Algorithm for Computing the Euler Number of an Image and its VLSI Implementation", *IEEE Thirteenth International Conference*, 2000, pp. 330-335.
- [19] L.R. Paul, "Thresholding for change detection", *Sixth IEEE International Conference on Computer Vision*, 1998, pp. 274-279.
- [20] M. Nixon, A. Agado, "Image Processing", Press Elsevier 2nd Edition, 2005.
- [21] W. Hongzhi, D. Ying, "An Improved Image Segmentation Algorithm Based on Otsu Method", *International Symposium on Photoelectronic Detection and Imaging*, Vol. 6625, 2007, pp. 196-202.
- [22] M. Galloway, "Texture analysis using gray level run lengths, *Computer Graphics and Image Processing*", Vol.4, No.2, 1975, pp. 172-179.
- [23] A. Amichi, P. Laugier, "Quantitative Texture Analysis and Transesophageal Echocardiography to Characterize the Acute Myocardial Contusion", *Open Medical Informatics Journal*, Vol. 3, 2009, pp. 13-19.
- [24] F. Lefebvre, M. Meunier, F. Thibault, P. Laugier, G. Berger, "Computerized ultrasound B-scan characterization of breast nodules", *Ultrasound in Medicine & Biology*, Vol.26, No.9, 2000, pp. 1421-1428.
- [25] N. Otsu, "A threshold selection method from grey-level histograms", *IEEE Trans. Syst. Man, Cybern*, Vol.8, 1978, pp. 62-66.
- [26] J.L. Rodgers, W.A. Nicewander, "Thirteen ways to look at the correlation coefficient", *The American Statistician*, Vol. 42, No.1, 1988, pp. 59-66.
- [27] M.M Mazid, ABM Shawkat Ali, K. S Tickle, "Improved C4.5 Algorithm for RuleBased Classification", *Proceedings of the 9th WSEAS international conference on Artificial intelligence, knowledge engineering and data bases*, 2010, pp. 296-301..
- [28] C.E. Osborn, "Statistical Application for Health in Formation Management", Press. Jones and Bartlett 2nd Edition, 2006.
- [29] W. L. Nowisnki, G. Qian, B. Prakash, I. Volkau, Q. Hu, A. Thirunavukarasu, N. Ivanov, A.S. Parimal, Yu Qiao1, A Ananthasubramaniam, Su Huang, V.M. Runge, N. J. Beauchamp, "Computer aided diagnosis: design and development of a system for stroke MR image processing", *Proceedings of the 2006 WSEAS Int. Conf. on Cellular & Molecular Biology, Biophysics & Bioengineering*, Athens, Greece, 2006, pp. 20-25.
- [30] A. Odogescu, I. Zetu, K. Martha, C. Sinescu, E. Petrescu, M. Negruiti, S. Talpos, E. Odogescu, "The Use of Biomedical Imaging for Computer-Aided Diagnosis and Treatment Planning in Orthodontics and Dentofacial Orthopedics", *Proceedings of the 4th WSEAS International conference on Biomedical electronics and biomedical informatics*, 2011, pp. 418-423.
- [31] D. Popescu, M. Nicolae, D. A. Crisan, N. Angelescu, "Computer Aided Diagnosis in Mammography based on Fractal Analysis", Proc. of the 5th WSEAS Int. Conf. on Non-Linear Analysis, Non-Linear Systems and Chaos, Bucharest, Romania, 2006, pp. 39-43
- [32] D.E. Maroulisa, M.A. Savelonasa, S.A. Karkanisb, D.K. Iakovidisa, N. Dimitropoulosc, "Computer-aided thyroid nodule detection in ultrasound images", *Computer-Based Medical Systems*, 2005. Proceedings. 18th IEEE Symposium, 2005, pp. 271-276.
- [33] U.U Ergun, S. Serhatlioglu, F. Hardalac, I. Guler, "Classification of carotid artery stenosis of patients with diabetes by neural network and logistic regression", *Computers in Biology and Medicine*, Vol. 34, No. 5, 2004, pp. 389-405.
- [34] H. Kahramanli, "A novel distance measure for data vectors with nominal feature values", *Proceedings of the European conference of systems, and European conference of circuits technology and devices, and European conference of communications, and European conference on Computer science*, 2010, pp. 265-267.
- [35] J. Paritsis, T.T. Veblen, J. M. Smith, A. Holz, "Spatial prediction of caterpillar (*Ormiscodes*) defoliation in Patagonian *Nothofagus* forests", *Landscape Ecol*, Vol. 26, 2011, pp. 791-803.

**Simona Moldovanu** – His birth place is Galati, Romania and her date of birth is 23.05.1972. She obtained her BSc degree in Mathematical Physics in 1999, and MSc degrees in IT in 2006 at "Dunarea de Jos" University of Galati. She is 3rd year PhD student in the field of Intelligent Systems for Diagnosis and Monitoring at Dunarea de Jos University from Galati. She is a Professor of Computer Science at "D.Motoc" High School Galati and has a teaching experience of 12 years. She has published 12 scientific papers as first author and co-author in national and international journals. Her current research interests are segmentation image features extraction, characterization and classification US image using CADi software.

**Luminita Moraru**- Her birthplace is Brasov, Romania and her date of birth is 21.03.1963. She obtained her BSc degree in 1986 from University of Bucharest and PhD in 1997 from University Dunarea de Jos of Galati. She is currently working as a Professor at University Dunarea de Jos of Galati and has a teaching experience of 21 years. Authored and co-authored of more than 130 research journals in national and international conferences and peer review journals. Her areas of interest are image processing, features extraction, segmentation and medical imaging processing. Prof. Dr. Moraru is a life member of Romanian Physical Society. She is member of the Board of External Examiners to adjudicate on the international PhD thesis- Annamalay University, India.

**Dorin Bibicu** – His birth place is Galati, Romania and his date of birth is 05.06.1976. He obtained his BSc degree in Mathematical Physics in 2000, and MSc degrees in IT in 2004 at "Dunarea de Jos" University of Galati. He is 2nd year PhD student in the field of Intelligent Systems for Diagnosis and Monitoring of Dunarea de Jos University from Galati. He is a Professor of Computer Science at "Dunarea" High School Galati and has a teaching experience of 11 years. He has published 5 scientific papers as first author and co-author in national and international journals. His current research interests are image processing, features extraction, medical imaging processing, artificial neural networks, CADi software.